

Enhanced Half-Metallicity in Edge-Oxidized Zigzag Graphene Nanoribbons

Oded Hod, Verónica Barone, Juan E. Peralta, and Gustavo E. Scuseria

Department of Chemistry, Rice University, Houston, Texas 77005-1892

(Dated: October 25, 2018)

We present a novel comprehensive *first-principles* theoretical study of the electronic properties and relative stabilities of edge-oxidized zigzag graphene nanoribbons. The oxidation schemes considered include hydroxyl, carboxyl, ether, and ketone groups. Using screened exchange density functional theory, we show that these oxidized ribbons are more stable than hydrogen-terminated nanoribbons except for the case of the etheric groups. The stable oxidized configurations maintain a spin-polarized ground state with antiferromagnetic ordering localized at the edges, similar to the fully hydrogenated counterparts. More important, edge oxidation is found to lower the onset electric field required to induce half-metallic behavior and extend the overall field range at which the systems remain half-metallic. Once the half-metallic state is reached, further increase of the external electric field intensity produces a rapid decrease in the spin magnetization up to a point where the magnetization is quenched completely. Finally, we find that oxygen containing edge groups have a minor effect on the energy difference between the antiferromagnetic ground state and the above-lying ferromagnetic state.

Low-dimensional carbon structures such as fullerenes¹ and carbon nanotubes² (CNTs) are promising candidates for building blocks of future nanoelectronic and nanomechanical devices.^{3,4} Made of a unique hexagonal carbon lattice confined to a quasi one-dimensional (1D) tubular structure, CNTs may be either semiconducting or metallic, depending on their diameter and chirality.⁵ Combined with their ballistic^{6,7,8,9,10,11} electronic transport characteristics, this opens exciting possibilities for the design of novel electronic components and interconnects with nanometer scale dimensions.

Recently, a new type of graphene-based material was experimentally realized.¹² Shaped as narrow stripes cut out of a single (or a few) layer(s) of graphite, these elongated materials were named graphene nanoribbons (GNR). Since they share the same hexagonal carbon lattice structure, GNRs and CNTs exhibit many similarities with respect to their electronic properties. However, the planar geometry of the ribbons allows for the application of standard lithographic techniques for the flexible design of a variety of experimental devices.^{12,13,14,15,16} The utilization of these established fabrication methods suggest the possibility of a controllable and reproducible fabrication of carbon based electronic components at the nanometer scale.

Despite the aforementioned similarities, there is a distinct difference between CNTs and GNRs. Unlike CNTs, GNRs present long and reactive edges prone to localization of electronic edge states and covalent attachment of chemical groups¹⁷ that can significantly influence their electronic properties. The importance of edge states was demonstrated for the case of arm-chair CNTs which present a metallic and non-magnetic^{3,5} character in their tubular form, but when unrolled into the corresponding zig-zag GNRs, they were predicted to become semiconducting^{18,19} with a spin polarized^{19,20,21,22,23,24,25} ground state. This ground state is characterized by opposite spin orientations of localized electronic states at the two edges of the GNR, which couple through the graphene back-

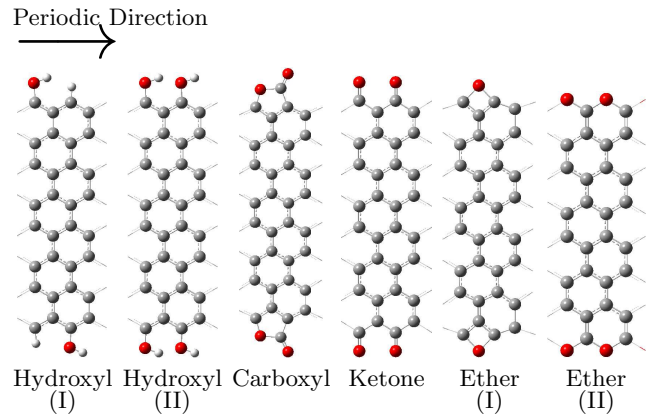


FIG. 1: Optimized unit cell geometries of different edge oxidation schemes studied in this work. Color code: red - oxygen atoms, gray - carbon atoms, white - hydrogen atoms.

bone via an antiferromagnetic (AF) arrangement of spins on adjacent atomic sites.

Recently, Son *et al.*¹⁹ have shown that upon the application of an electric field, an opposite local gating effect of the spin states on the two edges of the ribbon may occur. The in-plane field (perpendicular to the main axis of the ribbon) drives the system into a half-metallic state where one spin flavor exhibits a metallic behavior, while the opposite spins experience an increase in the energy gap. Apart from the interesting interplay between the electric field and the spin degree of freedom, this phenomenon is important from a technological standpoint since such a system could serve as a perfect spin filter in future nanospintronic devices.

Most of the theoretical studies on GNRs,^{18,20,21,22,23,24,25,26,27,28,29,30,31,32,33,34,35,36} including those on the half-metallic systems,^{19,37} address either bare or hydrogen terminated ribbons. Nevertheless, during standard GNRs fabrication processes, it

is commonly assumed that the ribbons edges become oxidized.^{38,39,40,41} Since many of the unique properties of GNRs are associated with edge states, edge chemistry in general and oxidation in particular, can significantly alter the electronic properties of the ribbons. It is the purpose of this letter to study, for the first time, the influence of edge oxidation on the relative stability, the electronic properties, and the half-metallic nature of zigzag graphene nanoribbons, from *first-principles*.

To this end, we study six different oxidation schemes of a 1.8 nm wide zigzag GNRs including hydroxylation, carboxylation, ketonation, and etheration, as shown in Figure 1. All the calculations presented in this work were carried out using periodic boundary conditions as implemented in the development version of the *Gaussian* suite of programs.^{42,43} Fully relaxed geometries were obtained using the PBE realization of the generalized gradient approximation^{44,45} and the polarized 6-31G** Gaussian basis set⁴⁶ for the non-magnetic (closed-shell) state. The electronic structures were then re-evaluated using the screened exchange hybrid density functional, HSE,^{47,48} which has been tested in a wide variety of materials and has been shown to accurately reproduce experimental band gaps^{49,50} and first and second optical excitation energies in metallic and semiconducting SWNTs.^{51,52} Furthermore, the inclusion of short-range exact-exchange in the HSE functional makes it suitable to treat electronic localization effects^{53,54,55,56,57} which are known to be important in this type of materials.^{18,19,20,21,22,23,24,25,26,27,28,37,58,59,60,61,62,63}

We start by studying the relative stability of the different oxidized ribbons. As these structures have different chemical compositions, the cohesive energy per atom does not provide a suitable measure for the comparison of their relative stability. Therefore, we adopt the approach customary used in binary phase thermodynamics to account for chemical composition and utilized previously to qualitatively analyze the relative stability of endohedral silicon nanowires⁶⁴ and arm-chair GNRs.³¹ Within this approach one defines a Gibbs free energy of formation δG for a GNR as:

$$\delta G(\chi) = E(\chi) - \chi_H \mu_H - \chi_O \mu_O - \chi_C \mu_C, \quad (1)$$

where $E(\chi)$ is the cohesive energy per atom of the GNR, χ_i is the molar fraction of atom i ($i=C,O,H$) in the ribbon, satisfying the relation $\sum_i \chi_i = 1$, and μ_i is the chemical potential of the constituent i at a given state. We choose μ_H as the binding cohesive energy per atom of the singlet ground state of the H_2 molecule, μ_O as the cohesive energy per atom of the triplet ground state of the O_2 molecule, and μ_C as the cohesive energy per atom of a single graphene sheet. This definition allows for a direct energy comparison between oxidized nanoribbons with different compositions, where negative values represent stable structures with respect to the constituents. It should be stressed that this treatment gives a qualitative assessment of the relative stability while neglecting thermal and substrate effects and zero point energy cor-

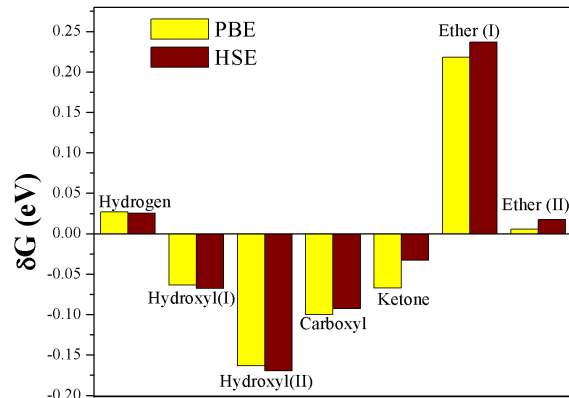


FIG. 2: Ground state relative stabilities of the different oxidation schemes studied (see Fig. 1) obtained via Eq. 1 at the PBE and HSE/6-31G** levels of theory. Negative values indicate stable structures with respect to the constituents.

rections.

In Figure 2 we present the relative stability of the ground states of the different oxidation schemes studied. The fully hydrogenated ribbons, as well as the two etherated ribbon configurations, are found to be less stable than their corresponding constituents. This is consistent with previous calculations on bare and hydrogen terminated GNRs.³¹ Nevertheless, the chemical passivation via hydroxylation, ketonization and carboxylation leads to considerable energetic stabilization of the structure of the ribbons. We find that the most stable structure corresponds to the fully hydroxylated ribbon. This enhanced stability is attributed to the hydrogen bonds formed between adjacent hydroxyl groups.

We now turn to study the electronic properties of the four most stable structures. In Figure 3 we show the ground state spin density of the fully hydrogenated, ketonated, hydroxylated and carboxylated structures, obtained with the HSE functional.⁶⁵ Similar to the fully hydrogenated GNR¹⁹, all the depicted oxidized structures exhibit a spin polarized ground state where the spin magnetization on the opposite edges of the ribbons are aligned anti-parallel. For the hydroxylated and the carboxylated ribbons, the presence of the oxidation groups slightly changes the absolute value of the spin polarization at the edge carbon atoms. However, the overall magnetization density resembles that of the fully hydrogenated GNR. A different picture arises for the ketonated system, where the oxygen p -electrons participate in the π system of the ribbon and therefore present considerable spin polarization, which results in a qualitatively different spin density map compared to that of the fully hydrogenated system.

In Table I we present the bandgaps and the energy differences per unit cell between the AF ground state and the above-lying ferromagnetic (FM) state (where the

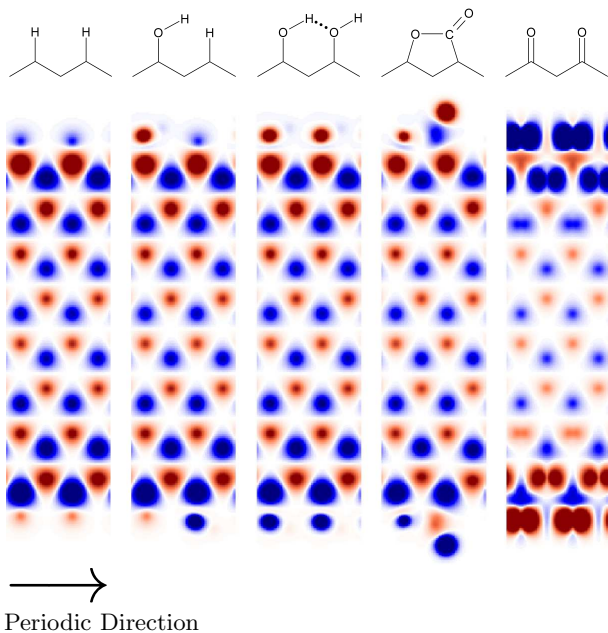


FIG. 3: Map of the HSE ground state spin densities 0.16 \AA above the surface of the ribbon for the four most stable oxidation schemes studied. The fully hydrogenated system is also included for comparison. Color code: Red α spin density; blue β spin density. A scheme of the different oxidation groups is presented for clarity.

TABLE I: HSE/6-31G** AF ground state bandgaps (eV) and energy differences between the FM and AF states (meV/unit cell) of the studied GNRs.

	E_g	$E_{FM} - E_{AF}$
Hydrogenated	1.05	42
Hydroxylated (I)	0.99	39
Hydroxylated (II)	0.90	38
Carboxylated	0.77	33
Ketonated	0.03	5

edges of the ribbon bare parallel spin polarization) for the hydrogenated, and stable oxidized structures. All studied oxidized structures, except for the ketonated ribbons, have a bandgap comparable to that of the fully hydrogenated ribbon, indicating that their electronic character is only slightly changed upon oxidation. Furthermore, the energy difference between the AF ground state and the FM state is above room temperature and similar to that of the hydrogenated ribbon. The ketonated ribbon, on the other hand, exhibits a vanishing bandgap and a very small energy difference between the AF ground state and the FM state, suggesting that it will be extremely difficult to observe the half-metallic nature of the ketonated ribbons even at low temperatures.

The analysis presented above suggests that, with the exception of the ketonated systems, all oxidation schemes have little effect on the electronic character of the GNRs

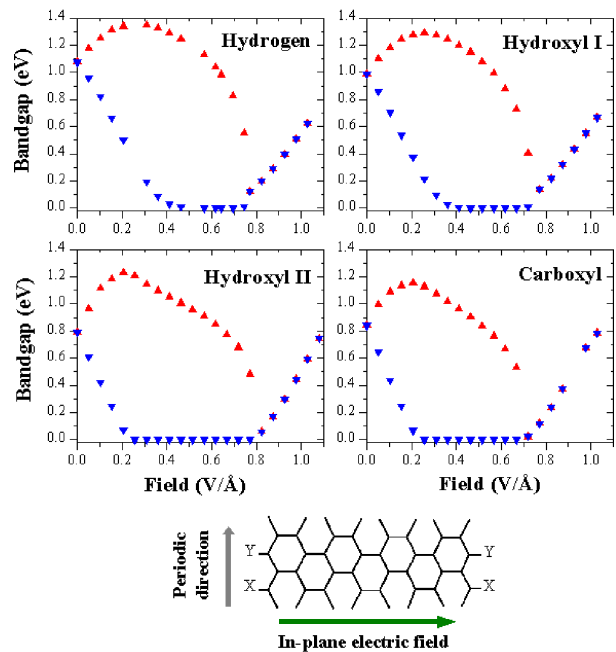


FIG. 4: Electric field effect on the spin polarized bandgap of oxidized GNRs. Red and blue triangles stand for the two different spin polarization bandgaps. The values are calculated using the HSE functional and the 3-21G basis set.⁶⁶ A scheme of the direction of the applied electric field is presented for clarity, where X and Y represent the oxidizing groups.

and therefore, one would expect these systems to behave as half-metals under the influence of an external electric field. To verify this assumption we have calculated the bandgap of the α and β spin channels as a function of the intensity of a transverse in-plane, uniform, and static electric field. In Figure 4 we plot the spin resolved bandgaps as a function of the field intensity for the fully hydrogenated, hydroxylated, and carboxylated ribbons. In the absence of an electric field, the α and β bandgaps are degenerate for all the studied systems. Upon the application of a low intensity electric field, a splitting occurs where the bandgap of one spin flavor increases and that of the opposite spin flavor decreases.¹⁹ The bandgap splitting increases monotonically with the field intensity up to a point where the system becomes half-metallic. Further increase in the external electric field intensity results in a decrease of the bandgap splitting up to a point where the systems become non-magnetic.

It is interesting to note that when the edges of the ribbon are fully or partially hydrogenated, the field intensity needed to switch the system to the half-metallic regime is 0.4 V/\AA and the range at which the half-metallic behavior is maintained is 0.3 V/\AA . Nevertheless, when the edges are fully oxidized, the system turns half-metallic at a lower field intensity (0.2 V/\AA) and the range of half-metallic behavior is doubled to 0.6 V/\AA . As shown previously in Ref. 19, the intensity of the field needed to achieve half-metallicity decreases with the ribbon width.

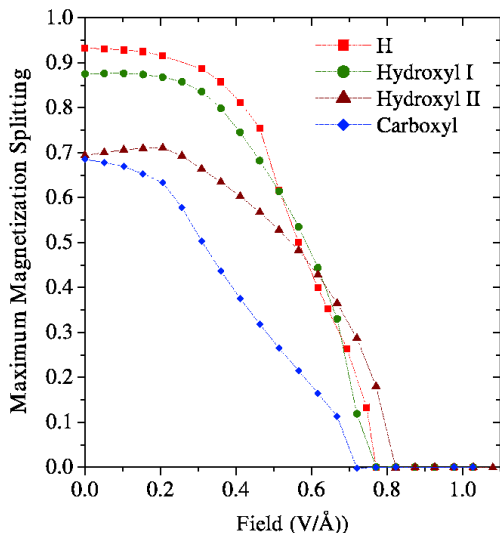


FIG. 5: Largest magnetization splitting between the two edges of the ribbon as a function of the electric field intensity. Calculations performed on the HSE/3-21G level of theory.

For a given width, the decrease of the field intensity needed to obtain the half-metallic behavior combined with the enhancement of the range at which this behavior is maintained, implies that edge oxidation is critical for the fabrication of robust and chemically stable spin filter devices out of zigzag GNRs.

It is relevant to investigate how the spin magnetization depends on the intensity of the applied electric field. To this end, in Figure 5 we present the maximum magnetization splitting as a function of the electric field, i.e. the difference between the maximum α and β Mulliken atomic spin densities.

For the four systems studied, at the low electric field regime, the field has minor influence on the magnetization splitting. Once the systems become half-metallic,

the magnetization drops sharply with the applied field up to a point where it fully quenches. An explanation for this behavior can be found by realizing that once the systems become half-metallic, the electric polarizability of the metallic spin channel increases considerably, allowing for a more effective spin compensation between the opposite edges of the ribbon. This results in an overall quenching of the spin magnetization. The electric field above which all the systems become diamagnetic is 0.7-0.8 V/Å for ribbons of about 1.8 nm wide.

In summary, we have presented a detailed study of the electronic properties and relative stabilities of several edge-oxidized zigzag GNRs. The structure of the oxidized ribbons is found to be stabilized with respect to the fully-hydrogenated counterparts except for the case of the etheric groups. Notably, all the stable oxidized structures studied maintain a spin polarized ground state with antiferromagnetic ordering. The above-lying ferromagnetic arrangement is expected to become accessible only beyond room temperature. Apart from the ketonated ribbons, all oxidized systems present a lower onset field and a wider electric field range for which half-metallic behavior is predicted. This suggests that edge oxidation is important for the design of efficient and robust spintronic devices based on GNRs. We have also shown that once the half-metallic state is reached, further increase of the external electric field produces a rapid decrease in the spin magnetization up to a point where all the systems become non-magnetic.

Acknowledgments

This work was supported by NSF Award Number CHE-0457030 and the Welch Foundation. Calculations were performed in part on the Rice Terascale Cluster funded by NSF under Grant EIA-0216467, Intel, and HP. O.H. would like to thank the generous financial support of the Rothschild and Fulbright foundations.

¹ H. W. Kroto, J. R. Heath, S. C. O'Brien, R. F. Curl, and R. E. Smalley, *Nature* **318**, 162 (1985).
² S. Iijima and T. Ichibashi, *Nature* **363**, 603 (1993).
³ M. S. Dresselhaus, G. Dresselhaus, and P. Avouris, *Topics in Applied Physics, Vol. 80* (Springer, Heidelberg, 2001).
⁴ R. H. Baughman, A. A. Zakhidov, and W. A. de Heer, *Science* **297**, 787 (2002).
⁵ R. Saito, G. Dresselhaus, and M. S. Dresselhaus, *Physical Properties of Carbon Nanotubes* (Imperial College Press, London, 1998).
⁶ S. J. Tans, M. H. Devoret, H. Dai, A. Thess, R. E. Smalley, L. J. Geerligs, and C. Dekker, *Nature* **386**, 474 (1997).
⁷ C. T. White and T. N. Todorov, *Nature* **393**, 240 (1998).
⁸ S. Frank, P. Poncharal, Z. L. Wang, and W. A. de Heer, *Science* **280**, 1744 (1998).
⁹ A. Bachtold, M. S. Fuhrer, S. Plyasunov, M. Forero, E. H. Anderson, A. Zettl, and P. L. McEuen, *Phys. Rev. Lett.* **84**, 6082 (2000).

¹⁰ C. T. White and T. N. Todorov, *Nature* **411**, 649 (2001).
¹¹ W. Liang, M. Bockrath, D. Bozovic, J. H. Hafner, M. Tinkham, and H. Park, *Nature* **411**, 665 (2001).
¹² K. S. Novoselov, A. K. Geim, S. V. Morozov, D. Jiang, Y. Zhang, S. V. Dubonos, I. V. Grigorieva, and A. A. Firsov, *Science* **306**, 666 (2004).
¹³ Y. Zhang, Y.-W. Tan, H. L. Stormer, and P. Kim, *Nature* **438**, 201 (2005).
¹⁴ C. Berger, Z. Song, X. Li, X. Wu, N. Brown, C. Naud, D. Mayou, T. Li, J. Hass, A. N. Marchenkov, E. H. Conrad, P. N. First, and W. A. de Heer, *Science* **312**, 1191 (2006).
¹⁵ K. S. Novoselov, Z. Jiang, Y. Zhang, S. V. Morozov, H. L. Stormer, U. Zeitler, J. C. Maan, G. S. Boebinger, P. Kim, and A. K. Geim, *Science* **315**, 1379 (2007).
¹⁶ M. Y. Han, B. Oezylmaz, Y. Zhang, and P. Kim, *cond-mat/0702511*.
¹⁷ R. Ramprasad, P. von Allmen, and L. R. C. Fonseca, *Phys. Rev. B* **60**, 6023 (1999).

- ¹⁸ K. Nakada, M. Igami, and M. Fujita, *J. Phys. Soc. Jap.* **67**, 2388 (1998).
- ¹⁹ Y.-W. Son, M. L. Cohen, and S. G. Louie, *Nature* **444**, 347 (2006).
- ²⁰ M. Fujita, K. Wakabayashi, K. Nakada, and K. Kusakabe, *J. Phys. Soc. Jap.* **65**, 1920 (1996).
- ²¹ K. Wakabayashi, M. Sigrist, and M. Fujita, *J. Phys. Soc. Jap.* **67**, 2089 (1998).
- ²² K. Wakabayashi, M. Fujita, H. Ajiki, and M. Sigrist, *Phys. Rev. B* **59**, 8271 (1999).
- ²³ K. Kusakabe and M. Maruyama, *Phys. Rev. B* **67**, 092406 (2003).
- ²⁴ A. Yamashiro, Y. Shimoi, K. Harigaya, and K. Wakabayashi, *Phys. Rev. B* **68**, 193410 (2003).
- ²⁵ H. Lee, Y.-W. Son, N. Park, S. Han, and J. Yu, *Phys. Rev. B* **72**, 174431 (2005).
- ²⁶ K. Nakada, M. Fujita, G. Dresselhaus, and M. S. Dresselhaus, *Phys. Rev. B* **54**, 17954 (1996).
- ²⁷ Y. Miyamoto, K. Nakada, and M. Fujita, *Phys. Rev. B* **59**, 9858 (1999).
- ²⁸ T. Kawai, Y. Miyamoto, O. Sugino, and Y. Koga, *Phys. Rev. B* **62**, 16349 (2000).
- ²⁹ N. M. R. Peres, A. H. Castro-Neto, and F. Guinea, *Phys. Rev. B* **73**, 195411 (2006).
- ³⁰ M. Ezawa, *Phys. Rev. B* **73**, 045432 (2006).
- ³¹ V. Barone, O. Hod, and G. E. Scuseria, *Nano Lett.* **6**, 2748 (2006).
- ³² Z. F. Wang, Q. Li, H. Zheng, H. Ren, H. Su, Q. W. Shi, and J. Chen, *Phys. Rev. B* **75**, 113406 (2007).
- ³³ C. T. White, J. Li, D. Gunlycke, and J. W. Mintmire, *Nano Lett.* **7**, 825 (2007).
- ³⁴ L. Brey and H. A. Fertig, *Phys. Rev. B* **75**, 125434 (2007).
- ³⁵ D. Gunlycke, D. A. Areshkin, and C. T. White, *Appl. Phys. Lett.* **90**, 142104 (2007).
- ³⁶ L. Pisani, J. A. Chan, B. Montanari, and N. M. Harrison, *Phys. Rev. B* **75**, 064418 (2007).
- ³⁷ Y.-W. Son, M. L. Cohen, and S. G. Louie, *Phys. Rev. Lett.* **97**, 216803 (2006).
- ³⁸ H. He, J. Klinowski, M. Forster, and A. Lerf, *Chem. Phys. Lett.* **287**, 53 (1998).
- ³⁹ A. Lerf, H. He, M. Forster, and J. Klinowski, *J. Phys. Chem. B* **102**, 4477 (1998).
- ⁴⁰ L. R. Radovic and B. Bockrath, *J. Am. Chem. Soc.* **127**, 5917 (2005).
- ⁴¹ S. Stankovich, D. A. Dikin, G. H. B. Dommett, K. M. Kohlhaas, E. J. Zimney, E. A. Stach, R. D. Piner, S. T. Nguyen, and R. S. Ruoff, *Nature* **442**, 282 (2006).
- ⁴² Frisch, M. J. et al., Gaussian, Inc., Pittsburgh, PA, *Gaussian Development Version, Revision B.07* (2003).
- ⁴³ K. N. Kudin and G. E. Scuseria, *Chem. Phys. Lett.* **283**, 61 (1998); K. N. Kudin and G. E. Scuseria, *Chem. Phys. Lett.* **289**, 611 (1998); K. N. Kudin and G. E. Scuseria, *J. Chem. Phys.* **111**, 2351 (1999).
- ⁴⁴ J. P. Perdew, K. Burke, and M. Ernzerhof, *Phys. Rev. Lett.* **77**, 3865 (1996).
- ⁴⁵ J. P. Perdew, K. Burke, and M. Ernzerhof, *Phys. Rev. Lett.* **78**, 1396 (1997).
- ⁴⁶ P. C. Hariharan and J. A. Pople, *Theoret. Chimica Acta* **28**, 213 (1973).
- ⁴⁷ J. Heyd, G. E. Scuseria, and M. Ernzerhof, *J. Chem. Phys.* **118**, 8207 (2003).
- ⁴⁸ J. Heyd, G. E. Scuseria, and M. Ernzerhof, *J. Chem. Phys.* **124**, 219906 (2006).
- ⁴⁹ J. Heyd and G. E. Scuseria, *J. Chem. Phys.* **121**, 1187 (2004).
- ⁵⁰ J. Heyd, J. E. Peralta, and G. E. Scuseria, *J. Chem. Phys.* **123**, 174101 (2005).
- ⁵¹ V. Barone, J. E. Peralta, M. Wert, J. Heyd, and G. E. Scuseria, *Nano Lett.* **5**, 1621 (2005).
- ⁵² V. Barone, J. E. Peralta, and G. E. Scuseria, *Nano Lett.* **5**, 1830 (2005).
- ⁵³ K. N. Kudin, G. E. Scuseria, and R. L. Martin, *Phys. Rev. Lett.* **89**, 266402 (2002).
- ⁵⁴ I. D. Prodan, J. A. Sordo, K. N. Kudin, G. E. Scuseria, and R. L. Martin, *J. Chem. Phys.* **123**, 014703 (2005).
- ⁵⁵ I. D. Prodan, G. E. Scuseria, and R. L. Martin, *Phys. Rev. B* **73**, 045104 (2006).
- ⁵⁶ P. J. Hay, R. L. Martin, J. Uddin, and G. E. Scuseria, *J. Chem. Phys.* **125**, 034712 (2006).
- ⁵⁷ D. Kasinathan, J. Kunes, K. Koepf, C. V. Diaconu, R. L. Martin, I. D. Prodan, G. E. Scuseria, N. Spaldin, L. Petit, T. C. Schulthess, and W. E. Pickett, *Phys. Rev. B* **74**, 195110 (2006).
- ⁵⁸ K. Kobayashi, *Phys. Rev. B* **48**, 1757 (1993).
- ⁵⁹ S. Okada and A. Oshiyama, *Phys. Rev. Lett.* **87**, 146803 (2001).
- ⁶⁰ Y. Niimi, T. Matsui, H. Kambara, K. Tagami, M. Tsukada, and H. Fukuyama, *Appl. Surf. Sci.* **241**, 43 (2005).
- ⁶¹ Y. Kobayashi, K. ichi Fukui, T. Enoki, K. Kusakabe, and Y. Kaburagi, *Phys. Rev. B* **71**, 193406 (2005).
- ⁶² Y. Niimi, T. Matsui, H. Kambara, K. Tagami, M. Tsukada, and H. Fukuyama, *Phys. Rev. B* **73**, 085421 (2006).
- ⁶³ Y. Kobayashi, K. ichi Fukui, T. Enoki, and K. Kusakabe, *Phys. Rev. B* **73**, 125415 (2006).
- ⁶⁴ T. Dumitrica, M. Hua, and B. I. Yakobson, *Phys. Rev. B* **70**, 241303 (2004).
- ⁶⁵ For some of the oxidation schemes, when using the PBE functional, we could not identify an anti-ferromagnetic arrangement and a non-magnetic ground state was found.
- ⁶⁶ J. S. Binkley, J. A. Pople, and W. J. Hehre, *J. Am. Chem. Soc.* **102**, 939 (1980).